

# High-frequency response and reversal dynamics of two-dimensional magnetic dot arrays

R. L. Stamps

*Department of Physics, University of Western Australia, Nedlands, WA 6907, Australia*

R. E. Camley

*Department of Physics, University of Colorado, Colorado Springs, Colorado 80933*

(Received 22 December 1998)

Results from simulations of dynamic response for finite arrays of single domain magnetic dots are presented. Linear and nonlinear high-frequency properties are discussed, and a relevance of these properties to magnetization reversal in switching processes is shown. Particular attention is given to effects of array geometry and applied field orientation. The direction of an applied field relative to the array sides is found to be important for determining degeneracies in the linear magnetostatic mode spectrum. Nonlinear microwave response is also examined by simulating effects of strong rf fields, and routes to chaos are found that depend on the field orientation. A connection between magnetostatic mode excitation and reversal times under a switching field is suggested. A consequence is a dramatic slowing of reversal rates for a range of dot packing densities. [S0163-1829(99)02438-8]

## I. INTRODUCTION

The technology to fabricate high quality magnetic wire and dot structures with physical extensions on the submicrometer and nanometer length scale has been perfected to a remarkable degree in the past few years.<sup>1,2</sup> The extreme precision with which elements and arrays can be constructed opens many fascinating possibilities for studying how particle and array geometries affect magnetization processes.<sup>3</sup> As a consequence, old questions out of fine particle magnetism are being re-examined for regular arrays of interacting particles. Of these questions, important considerations for applications include aspects of switching and reversal times.<sup>4</sup> For these types of technological application, the relevant processes usually involve some type of nonlinear dynamic response to a driving field.<sup>5</sup>

In terms of nonlinear dynamics, insulating ferrimagnets, such as yttrium iron garnet (YIG) have served as model systems in studies using high power driven resonance experiments. This is an aspect usually ignored for ferromagnetic metals because of large eddy current losses.<sup>6</sup> Eddy current losses can be significantly reduced for ferromagnetic metals in small dot form, making patterned systems interesting candidates for new studies of nonlinear dynamics. Geometrically patterned arrays offer an interesting variant on previous resonance studies by allowing modification of the underlying interactions through details of the array geometry construction. The simplest modification of the interaction is to vary the spacing between magnetic elements, which affects the strength of the dipolar interaction. Other variations involve the orientation of the applied field, the symmetry of the array, and the size of the array.<sup>7</sup>

The size and spacing of the magnetic elements are shown to affect the magnetostatic modes observable in magnetic-resonance experiments through interparticle dipolar coupling. If the dot sizes are large enough, and the spacing between them small enough, the strength of the dipolar interactions can be comparable to magnetocrystalline anisotropy fields.<sup>7</sup>

In the same way that demagnetization effects are very important for understanding spin-wave excitations and spin resonance in ferromagnets, the dipolar field in an array of magnetic elements can affect the magnetostatic modes associated with the array. In this way the shape of the array plays a role analogous to that of shape anisotropies in films. In the first part of this paper, this sensitivity to details of array geometry and applied field orientation is explored for linear magnetostatic modes in finite arrays of circular dots.

The second part of this paper deals with the response of magnetic dot arrays to high power rf driving fields. The consideration here is that nonlinear processes involving interactions between linear magnetostatic modes are strongly dependent on mode symmetry and wavelength.<sup>9,10</sup> A study of how these processes occur in magnetic dot arrays is therefore interesting because the character of the allowed linear magnetostatic modes are controlled by the array geometry. This aspect of nonlinear response of magnetic arrays is examined through numerical simulations of the response of a dot array to a large amplitude oscillating driving field. Magnetostatic interactions between dots are shown to strongly affect the nonlinear response of an array.

The final part of the paper proposes an interesting connection between magnetic reversal under applied switching fields and magnetostatic excitations between particles in the dot array. Reversal of magnetization of a small particle involves highly nonlinear dynamics of the magnetic moment.<sup>8</sup> If the particles are coupled, then excitations in the coupled array will be involved and can affect the rate at which reversal takes place. A curious and technologically relevant result is that the switching time for an interacting array of magnetic dots is very sensitive to the array spacing and particle size. A maximum switching time is found for certain lattice spacings. The maximum appears to be the consequence of a resonant effect with the band of magnetostatic excitations.

The paper is organized as follows. In Sec. II, the linear dynamic response of a magnetic dot array is examined using

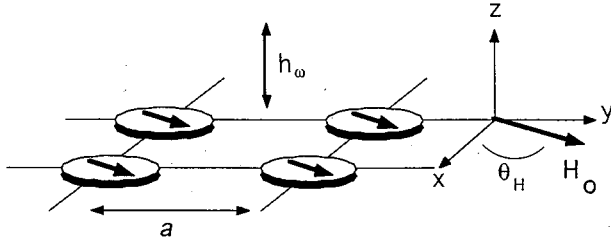


FIG. 1. Array geometry. The dots are positioned on a square array with spacing  $a$ . A static magnetic field is applied at an angle  $\theta_H$  from the  $x$  axis and a time varying driving field is applied normal to the array plane in the  $z$  direction.

a numerical integration scheme. In this section, effects of array geometry studied. In Sec. III, response to strong driving fields is examined and the dependence of nonlinear dynamic behavior on the array spacing is studied, particularly in regards to the onset of chaotic behavior. Consequences for high-speed switching behavior are also investigated. A summary is given in Sec. IV.

## II. LINEAR MAGNETOSTATIC EXCITATIONS

The calculation method is to numerically integrate the time dependent Landau-Lifshitz equations of motion for a large array of interacting magnetic dots.<sup>7</sup> This has an advantage over analytic approaches in that relaxation and response can be examined as easily in the linear response regime as in the nonlinear regime. The disadvantage is that the size of the system that can realistically be studied is limited. Regardless, for the present purposes of illustrating some of the possibilities present for experiments with patterned magnetic arrays, the numerical simulation method is ideal.

### A. Simulation method

Single domain, cylindrically shaped particles are assumed. These magnetic ‘‘dots’’ are assumed to be small, uniformly magnetized, and behave as point dipoles. The size of the particles is therefore small compared to the exchange length. This is a reasonable restriction for the purposes of this paper because the low-frequency dynamic response of such small particles is governed by the net magnetic moment of each particle. In all cases considered, the temperature is supposed to be low enough to ignore superparamagnetic behavior. The small size of the particles also implies that high-energy exchange modes do not contribute to the rf frequency response. Contributions from these modes are therefore neglected.

The magnetic dots are arranged on a rectangular array at positions  $\mathbf{i}$  associated with position vectors  $\mathbf{r}_i = \mathbf{x}na + \mathbf{y}ma$  where  $a$  is the array lattice spacing and  $n$  and  $m$  are integers. The geometry is shown in Fig. 1. An external applied field  $H_0$  is positioned in the plane of the array at an angle  $\theta_H$  measured from the  $y$  edge of the array. A driving field  $h_\omega$  is aligned normal to the array plane. The dot magnetic moments are aligned in the film plane at equilibrium.

The classical equation of motion of a dot magnetic moment  $\mathbf{m}$  at position  $\mathbf{r}$  in the array is

$$\partial \mathbf{m}_i / \partial t = \gamma \mathbf{m}_i \times \mathbf{H}_i - \alpha \mathbf{m}_i \times \dot{\mathbf{m}}_i \times \mathbf{H}_i. \quad (1)$$

Here  $\gamma$  is the gyromagnetic ratio and  $\alpha$  controls the rate of dissipation. This form of dissipation is chosen to conserve the magnitude of the dot moment as  $|\mathbf{m}|/V = M$  where  $V$  is the dot volume. The field  $\mathbf{H}_i$  is an average effective field acting at position  $\mathbf{i}$ :

$$\mathbf{H}_i = \mathbf{x}H_0 \cos \theta_H + \mathbf{y}H_0 \sin \theta_H + \mathbf{z}[(2K/M^2)m_{zi} + h_\omega \cos \omega t] - \mathbf{d}_i. \quad (2)$$

Contributions to  $\mathbf{H}_i$  are the static applied field, anisotropy  $K$ , and dipolar interactions with the other magnetic dots, represented by the field  $\mathbf{d}$ .

The shape and magnetocrystalline contributions to the anisotropies in the dots are described by a single uniaxial anisotropy  $K$  with easy axis directed normal to the dot array plane. The dipole field  $\mathbf{d}_i$  due to all the other dots in the array is also time dependent and has the form

$$\mathbf{d}_i = \sum_j \left[ \frac{\mathbf{m}_j}{r_{ij}^3} - 3 \frac{\mathbf{r}_i \cdot \mathbf{m}_j}{r_{ij}^5} \mathbf{r}_i \right]. \quad (3)$$

Equation (1) can be written in spherical coordinates involving only two degrees of freedom for each dot. The problem is then treated by solving the set of  $2N^2$  coupled equations for a square dot array of dimension  $N$  numerically using a second-order Runge-Kutta method. In this technique, the time evolution of each dot in the array is calculated over a small time interval  $\Delta t$ . Parameters for the calculations are in units reduced by the magnetization of the dot material  $M$ . The unit of time in the reduced units is  $\gamma M t$ . In these units, convergent solutions can be found with  $\Delta t$  on the order of 0.005 within 10 000 time steps for small arrays ( $N$  around 4).

The dipole strength is determined by the physical structure of the array and is characterized by the ratio of dot volume to array cell volume, denoted by  $h_d$ . In the reduced units used in this paper,  $h_d \propto V/r^3$ . This means the strength of the interaction is determined by  $h_d = \pi h R^2/a^3$ , where  $h$  and  $R$  are the height and radius of a dot cylinder, and  $a$  is the center to center distance between nearest-neighbor dots. Unless otherwise specified, a value of  $h_d = 1.0$  is used.

It is also useful to note that the equilibrium ‘‘ground-state’’ configuration is automatically generated when dissipation is included because the system naturally tends toward the static configuration over time as the system dissipates its kinetic energy and settles into an equilibrium configuration. This feature has been used to study quasistatic properties of a number of different systems.<sup>11</sup>

### B. Linear excitations

In direct analogy to magnetostatic modes confined in a piece of ferromagnetic material, magnetostatic excitations can exist confined to an array of magnetic dots. The modes exist as standing modes in analogy to magnetostatic spin waves confined to finite films. The frequencies depend on  $h_d$ ,  $K$ , and the magnitude and orientation of  $H_0$ . Excitation frequencies are calculated using the numerical simulation two different methods. One method, which gives a direct measure of the absorption measured using ferromagnetic resonance, is to examine amplitudes of the spin precession

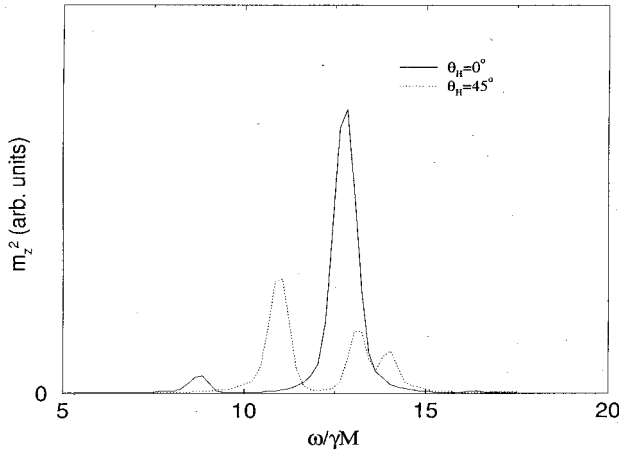


FIG. 2. Linear response as a function of frequency. A small driving field ( $h_\omega=0.01$ ) is applied parallel to the edge of an array and also along a diagonal. The array contains nine dots and is in-plane magnetized. The width of the peaks is due to damping and the existence of several nearly degenerate modes. The arrows correspond to the resonance frequencies given by the approximation of Eq. (5).

when driven by the  $h_\omega$  field in Eq. (2). A second method is to analyze the frequency dependence of a system after a small disturbance to the equilibrium orientation has been made.

The first method can be used to define a frequency dependent response  $m_z^2$  which shows structure at frequencies that represent resonances of the system:

$$m_z^2(\omega) = \frac{1}{N^2} \left( \sum_i m_{zi} \right)^2. \quad (4)$$

A numerical scan of  $m_z^2$  for small amplitude driving fields and different driving frequencies  $\omega$  has peaks at frequencies corresponding to excitations of magnetostatic modes in the array.

An example calculation for an array of nine dots is shown in Fig. 2. The anisotropy  $K$  is set to  $-4\pi$  representing an in-plane orientation of the magnetization at equilibrium. The plot shows the response  $m_z^2$  with a damping  $\alpha/\gamma M^2 = 0.001$ . Results for a static field of magnitude  $H_0/M = 2$  applied parallel to the array edge, for  $\theta_H = 0$ , and along a diagonal, for  $\theta_H = 45^\circ$ , are shown. The amplitude of the driving field is small, with  $h_\omega = 0.01$ , so that only linear response is probed.

The width of the peaks is due partly to damping, but the main contribution to linewidth comes from excitation of several nearly degenerate modes. The directions  $\theta_H = 0$  and  $45^\circ$  are high symmetry and many excitations can exist with nearly the same frequency. The degeneracy can be lifted by increasing the strength of the coupling and by choosing field orientations in low-symmetry directions.

It is useful to note that the frequency of the resonance mode for the dot array is approximated very well as the ferromagnetic resonance frequency:

$$\omega/\gamma = \{(H + D_x - D_y)[H + D_x - D_z + (2K/M)]\}^{1/2}. \quad (5)$$

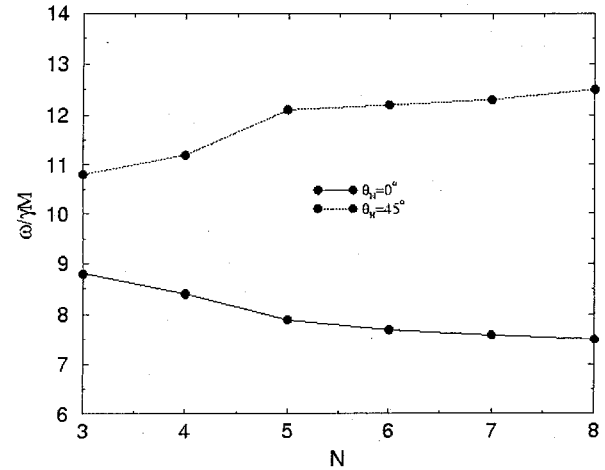


FIG. 3. Magnetostatic mode frequency as a function of array size. The static field is applied along an array edge for the frequencies along the solid line, and along a diagonal for frequencies along the dotted line. The difference between the two frequencies decreases with array size  $N$  but approaches a limiting nonzero value for large  $N$ .

The demagnetization factors  $D_v$  are *not* demagnetization factors for the individual dots, but instead depend on the array geometry. These factors depend on the orientation of the dot magnetic moments, and also on the dot size and array size and geometry. In general they will also depend on position within the array. For comparison of Eq. (5) to the simulation results, the factors were approximated by summing the dipolar fields produced by a static arrangement of dots acting at the center of the array. The corresponding frequencies were calculated according to Eq. (5). Results for the case considered in Fig. 2 are shown by the arrows.

The good agreement between the approximation of Eq. (5) and the numerical calculation is due to the close analogy between shape anisotropies in ferromagnets and the ‘‘shape anisotropies’’ produced by the geometry of the magnetic dot array. Both are demagnetizing effects that reflect the boundaries of the magnetizable material. The effects are very significant for small arrays and still exist even for large arrays.

This is illustrated in Fig. 3 where the mode frequencies corresponding to the low-frequency peak in Fig. 2 are shown as a function of array size. The static field is applied along an array edge for the solid line and along a diagonal for the dotted line. The frequencies were determined by analyzing the fourier spectrum obtained using the second method mentioned above. In this method, the equilibrium configuration for the magnetic moments is found by letting the simulation run until all the kinetic energy of the precessing moments is dissipated. The transient behavior of a dot in the array is then studied in response to a small perturbation of a dot moment away from equilibrium. This approach does not require a driving field and so  $h_\omega$  is set to zero.

The response frequencies obtained from the analysis give the fine structure of the peak responses shown in Fig. 2, and only the frequency of the lowest frequency excitation corresponding to the small peak in Fig. 2 is shown in Fig. 3. The difference in frequencies between the two field orientations indicates the importance of array shape on the linear re-

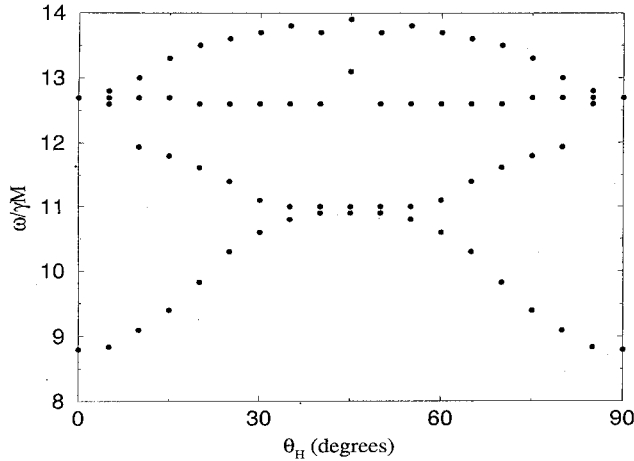


FIG. 4. Magnetostatic mode frequency as a function of field orientation. The frequencies of the lowest frequency modes in Fig. 2 for a nine-dot array are shown for a constant field aligned along directions specified by  $\theta_H$ . The fourfold symmetry of the underlying array appear in the frequencies for all lattice sizes. Note the lifting of degeneracies for field directions along low-symmetry axes.

sponse of the array. The difference decreases as the size of the dot array does, but approaches a limiting value for large  $N$ .

This behavior is in direct analogy to the effects of shape demagnetizing fields on conventional ferromagnetic resonance. Array shape demagnetizing effects also appear as a field orientation dependence of the magnetostatic mode frequencies on  $\theta_H$ . This is illustrated by the calculations shown in Fig. 4 where mode frequency is given as a function of field orientation. In this figure, the frequencies of peaks in the  $m_z^2$  response are plotted for a nine-dot array with a constant field aligned along directions specified by  $\theta_H$ . Note that additional magnetostatic excitations exist at higher frequencies, but do not generate a significant response in the average of Eq. (4) and can therefore not be observed using resonance techniques.

The fourfold symmetry of the underlying array appears in the frequencies for all lattice sizes. This may account for similar orientation dependence observed recently in spin-wave scattering experiments from square arrays.<sup>12</sup> Note that the points plotted in Fig. 4 represent peaks which actually represent contributions from several nearly degenerate modes. This gives seeming discontinuities and structure to the frequencies when plotted against  $\theta_H$  as the degeneracies are lifted through mode-mode interactions. The interactions occur when the field is near a high-symmetry direction. As the orientation angle of the field approaches these directions, the frequencies of some modes approach one another and hybridization occurs because of the dipole interaction.

### III. NONLINEAR RESPONSE AND SWITCHING TIME

The additional degree of freedom available in the dot geometry for varying dynamic demagnetizing fields was shown in Sec. II to strongly affect linear magnetostatic modes. The ability to control the strength of the interparticle interaction

by adjusting dot spacing and size can be especially important for nonlinear magnetostatic excitations. In this section, the effects are shown to be quite spectacular in terms of nonlinear magnetostatic response, where various nonlinear resonance phenomena, including approaches to chaos dynamics, are found to be strongly dependent on interdot interactions.

#### A. Driven response

The following system is considered in order to highlight the role of interdot coupling. A square array of magnetic dots is chosen where each dot has a uniaxial anisotropy that favors orientation of the dot magnetic moment *out* of the array plane. A time dependent circular polarized driving field with strength  $h_\omega$  and frequency  $\omega$  is applied in the plane of the array. The driving field is large enough to cause the dot magnetic moments to precess about an in-plane axis. This situation corresponds to a time dependent “switching” field which causes the moments to reverse direction relative to the particle easy axis. The key observation here is that if there are no dipolar interactions (corresponding to large array spacing or low moment dots), then the system is integrable and there is no chaotic behavior.<sup>9</sup>

An analysis can be done in terms of angles  $\theta$  and  $\phi$  specifying the instantaneous position of a dot’s magnetic moment. In the absence of interdot coupling, fixed points can be determined analytically in terms of the angles  $\theta$  and  $\phi$ . The location and classification of these points depend sensitively

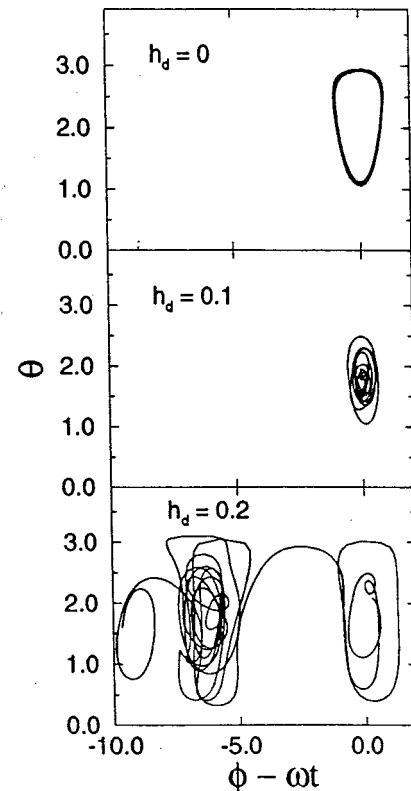


FIG. 5. Orbits around a fixed point for a nine-dot square out-of-plane magnetized dot array. The position of the array center dot moment is shown in terms of angle  $\theta$  and  $\phi$ .  $\theta$  is measured from the normal to the array plane and  $\phi$  is the in-plane angle. The system is not chaotic in the absence of dipolar interactions, but develops a chaotic transient response as the dipole coupling is increased ( $h_d$ ).

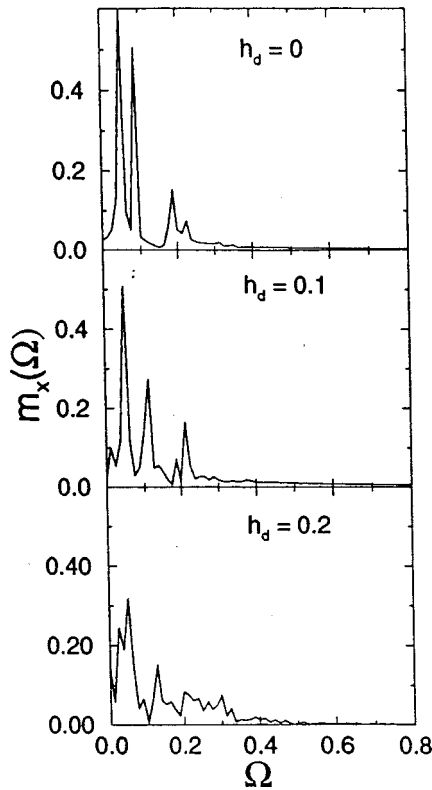


FIG. 6. Frequency spectrum of an in-plane component of the array average moment for the system in Fig. 5. Additional frequencies appear in  $m_x$  as the dipole coupling is increased.

on the ratios of  $\omega/K$  and  $\omega/h_\omega$  and exist at  $2\pi$  intervals in  $\phi$ . Complete discussions in the case of zero interdot coupling are given in Refs. 9 and 13.

The effects of interdot interactions is significant in this system and illustrated in Fig. 5. In this figure trajectories of the magnetic dot moment are shown in terms of position angles  $\phi$  and  $\theta$ . For convenience, a reference frame is chosen that rotates with the circularly polarized driving field.<sup>13</sup>

The trajectory around one of the stable fixed points is shown in the top left panel of Fig. 5 for the case of no dipolar interdot coupling ( $h_d=0$ ) in a nine-dot square array. There is no static applied field and the orbit is shown for the dot moment in the center of the array. A small dissipation is included with the value  $\alpha/\gamma=0.001$ ,  $\omega/K=0.6$ , and  $\omega/h_\omega=0.3$ . The frequency spectrum of an in-plane component of the average array magnetization  $m_x$  is shown in the top panel of Fig. 6 for the same system and parameters.

The effect of increasing the dipolar coupling (by decreasing the dot spacing, for example), is shown in the lower two panels of Figs. 5 and 6. The middle panel of Fig. 5 shows the behavior of the center array moment for  $h_d=0.1$ . Additional periods appear, corresponding with the appearance of additional frequencies in the spectrum for  $m_x$  shown in the middle panel of Fig. 6.

The bottom panel of Fig. 5 shows a portion of a chaotic orbit for  $h_d=0.2$ . The trajectory switches between different basins, although eventually appears to settle into a limit cycle after long times (not shown here). A numerical calculation of the Lyapunov exponent over long time periods shows that the exponent hovers around a maximum positive

value initially, but eventually tends toward zero at long times. This is analogous to transient chaotic behaviors discussed for nonlinear resonance behavior in YIG materials.<sup>10</sup>

The orbits shown in Figs. 5 and 6 were for the center dot moment. The amplitudes and orbits of moments for the remaining dots were interesting from the point of view of finite-size effects and localization. The response to large amplitude driving fields near the peak frequencies of the two linear resonance peaks of Fig. 2, for example, differed in terms of which dot moments exhibited the largest amplitude motion. Driving near the low-frequency peak produced large amplitude response and reversal of the center moments whereas driving near the high-frequency peak produced large amplitude response of the edge spins. It is interesting to note that the reversal of moments in this manner happens extremely fast because it is dynamically driven rather than dissipatively driven. The reversal time is thus determined by  $\gamma$ , not  $\alpha$ , and can be on the order of a precession time.

### B. Switching time of coupled arrays

Another kind of nonlinear dynamic process in magnetic systems is reversal. The reversal of magnetization in fine particles is important for various applications and has been studied extensively for fine single-domain particles.<sup>4,5</sup> The effects of coupling in terms of high-frequency behavior has not been discussed and turns out to have surprising consequences.

The essential feature is that the nonlinear magnetostatic modes supported by the array system are responsible for the chaotic response described above and also impact switching processes. This can be illustrated with the model system of perpendicular moments used above. In this problem, the array is initially oriented with each moment along the positive  $z$  direction (along the easy axis of the anisotropy). At  $t=0$ , a reverse field is applied along the  $-z$  direction and the time measured for the spins to rotate into the field direction.

The ‘‘switching’’ time  $\tau_s$  is defined as twice the time between the application of the reversal field and the time at which the average moment of the array in the  $z$  direction vanishes. The effect of coupling on this switching time is

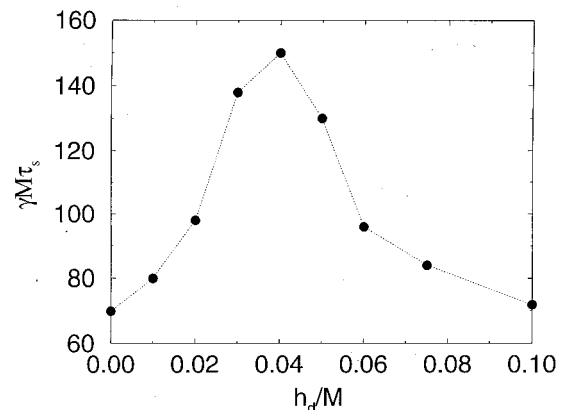


FIG. 7. Switching time as a function of interparticle coupling for a nine-dot square. Here  $K/M=1.1$ ,  $b/h=0.08$ , and  $\gamma/\alpha=0.07$  for each particle. The switching rate increases dramatically for a small range of coupling strengths  $h_d$ . For  $h_d/M$  near 0.04, coupled oscillations are excited in the array that slow the reversal process.

shown in Fig. 7 for a nine-dot square array as a function of coupling strength  $h_d$ . The parameters are  $K/M=1$ ,  $H_o/M=1.1$ , and  $\gamma/\alpha=0.07$  for each particle. In all cases the applied field has a small component ( $H_{ox}/H_{oz}=0.08$ ) along the  $x$  direction. This is necessary for the classical dynamics approach of this theory because otherwise the moments would never reverse when starting exactly from equilibrium.

The surprising feature is the distinct maximum in the switching time near  $h_d/M=0.04$ . The switching time for this value is increased by nearly a factor of 3 from times for values of  $h_d$  above or below this value. We believe the curious maximum occurs due to excitation of nonlinear magnetostatic oscillations in the dot array.

#### IV. SUMMARY AND CONCLUSIONS

The high-frequency linear and nonlinear response of an array of magnetic dots was examined using a numerical integration scheme. The theory allowed for precession and dissipation effects. Linear magnetostatic excitations were found for the array and shown to depend on dot array geometry and spacing. The shape of the array introduced shape anisotropy effects analogous to those known for magnetic resonance in ferromagnets. Peaks in the response were composed of nearly degenerate magnetostatic excitations with frequencies strongly dependent on the orientation of the applied field relative to the array directions. The excitations form a band whose width is determined by the strength of the dipolar interaction and is thus sensitive to the size of the magnetic particles and the array spacing. The magnetostatic excita-

tions can be measured using low-frequency, long-wavelength techniques such as light scattering or ferromagnetic resonance.

Nonlinear effects were studied for a particle array of perpendicularly oriented moments. The moments were driven by a field oriented such that the moments rotated into and out of the array plane. A threshold was found for the interdot coupling above which the system displays chaotic dynamics with a positive Lyapunov exponent. Localization of modes was also found in finite array geometries for certain frequencies. This mode localization resulted in particular dots exhibiting large amplitude switching at rates much faster than would be possible through usual damping controlled rotation. In this sense, the nonlinear processes can facilitate switching in finite arrays.

Finally, switching processes in coupled arrays were studied by examining the effect of applying a reversal field. The dynamic response was characterized in terms of a switching time that showed a dramatic increase for a small range of coupling strengths. The increase is thought to be due to the excitation of low-frequency oscillations in the dot array. This corresponds to a large slowing of the reversal process that could be realized for a restricted range of particle sizes and spacings in an array of magnetic particles.

#### ACKNOWLEDGMENTS

R.L.S. acknowledges support under ARC Small Grant and NSF Grant No. DMR-9703783. R.E.C. acknowledges support under ARO Grant No. DAAH04-94-G-0253.

<sup>1</sup>D. D. Awschalom and D. P. DiVincenzo, *Phys. Today* **48** (4), 43 (1995).

<sup>2</sup>M. Hehn, K. Ounadjela, J. P. Bucher, F. Rousseaux, D. Decanini, B. Bartenlian, and C. Chappert, *Science* **272**, 1782 (1996).

<sup>3</sup>R. L. Stamps and K. Ounadjela, in *Handbook of Nanostructured Materials and Nanotechnology*, edited by H. S. Nalwa (Academic, New York, 1999).

<sup>4</sup>R. Kikuchi, *J. Appl. Phys.* **27**, 1352 (1956).

<sup>5</sup>W. K. Hiebert, A. Stankiewicz, and M. R. Freeman, *Phys. Rev. Lett.* **79**, 1134 (1997).

<sup>6</sup>R. E. Camley, T. J. Parker, and S. R. P. Smith, *Phys. Rev. B* **53**, 5481 (1996).

<sup>7</sup>R. L. Stamps and R. E. Camley, *J. Magn. Magn. Mater.* **177-181**, 813 (1998).

<sup>8</sup>F. Waldner, D. R. Barberis, and H. Yamazaki, *Phys. Rev. A* **31**, 420 (1985).

<sup>9</sup>X. Y. Zhang and H. Suhl, *Phys. Rev. A* **32**, 2530 (1985).

<sup>10</sup>S. M. Rezende, O. F. de Alcantara Bonfin, and F. M. de Aguiar, *Phys. Rev. B* **33**, 5153 (1986).

<sup>11</sup>R. E. Camley, B. V. McGrath, R. J. Astalos, R. L. Stamps, J.-V. Kim, L. Wee, *J. Vac. Sci. Technol. A* **17**, 1335 (1999).

<sup>12</sup>B. Hillebrands, C. Mathieu, M. Bauer, S. O. Demokritov, B. Bartenlian, C. Chappert, D. Decanini, F. Rousseaux, and F. Carcenac, *J. Appl. Phys.* **81**, 4993 (1997).

<sup>13</sup>X. Y. Zhang, Ph.D. dissertation, University of California, San Diego, 1987.